Rapid Communications

# Existence of a critical canting angle of magnetic moments to induce multiferroicity in the Haldane spin-chain system $Tb_2BaNiO_5$

Ram Kumar,[1] Sudhindra Rayaprol,[2] Sarita Rajput,[3] Tulika Maitra,[3] D. T. Adroja,[4,5] Kartik K. Iyer,[1] Sanjay K. Upadhyay,[1] and E. V. Sampathkumaran[1,*]

[1]*Tata Institute of Fundamental Research, Homi Bhabha Road, Colaba, Mumbai 400005, India*

[2]*UGC-DAE-Consortium for Scientific Research, Mumbai Centre, BARC Campus, Trombay, Mumbai 400085, India*

[3]*Department of Physics, Indian Institute of Technology, Roorkee-247667, Uttarakhand, India*

[4]*ISIS Pulsed Neutron and Muon Source, STFC Rutherford-Appleton Laboratory, Harwell Campus, Didcot, Oxfordshire 011 0QX, United Kingdom*

[5]*Highly Correlated Matter Research Group, Physics Department, University of Johannesburg, P.O. Box 524, Auckland Park 2006, South Africa*

(Received 30 November 2018; revised manuscript received 11 February 2019; published 29 March 2019)

We report an unusual canted magnetism due to $3d$ and $4f$ electrons, occupying two different crystallographic sites, with its consequence to electric dipole order. This is based on neutron powder diffraction measurements on $Tb_2BaNiO_5$ (orthorhombic, *Immm* centrosymmetric space group), exhibiting Néel order below ($T_N$ =) 63 K, to understand multiferroic behavior below 25 K. The magnetic structure is made up of Ni and Tb magnetic moments, which are found to be mutually canted in the entire temperature range below $T_N$, though collinearity is seen within each sublattice, as known in the past. First-principles density functional theory calculations (GGA + SO and GGA + U + SO approximations) support such a canted ground state. The intriguing finding, being reported here, is that there is a sudden increase in this Tb-Ni relative canting angle at the temperature (that is, at 25 K) at which spontaneous electric polarization sets in, with bond distance and bond angle anomalies. This finding emphasizes the need for a new spin-driven polarization mechanism—that is, a critical canting angle coupled with exchange striction—to induce multiferroicity in magnetic insulators with canted spins.

DOI: 10.1103/PhysRevB.99.100406

The study of the materials exhibiting multiferroicity—a phenomenon arising from a coupling between two ferroic orders which were historically considered to be mutually exclusive, e.g., ferroelectric and magnetic order parameters—is an active topic of research [1–14]. Over the past decade, various theoretical models have been proposed to explain such a spin-driven ferroelectricity [see, for instance, [1,13–24]], with the magnetism from transition-metal ions commonly known to trigger such a phenomenon. While models based on exchange striction have been applied to collinear (CL) spin systems, Dzyaloshinski-Moriya interaction (DMI), which is asymmetric exchange interaction ($S_i \times S_j$) between spins at different sites, has been believed to govern multiferroic behavior for the materials with noncollinear (NCL) magnetic structures (that is, for a spatially rotating magnetic structure). Conventional DMI-based models, such as the Katsura, Nagaosa, and Balatsky (KNB) model [16], are applicable to those in which the normal vector of the spin spiral plane is *perpendicular* to the propagation vector (as in a cycloidal magnetic structure) and does not involve lattice degree of freedom. The DMI interaction via a third ligand ion was also proposed by Sergienko and Dagotto [17] to lead to electric polarization due to displacement of the ligand in transition-metal systems in which the superexchange mechanism mediates magnetic ordering. However, such DMI-based models could not explain the origin of ferroelectricity in proper screw-type magnetic systems—as in delafossites (e.g., $CuCrO_2$) [18]—in which the normal vector of the spins at two different sites is *parallel* to the propagation vector. Among various other theories to describe canted-spin-caused ferroelectricity [19–24], a "local" approach by Kaplan and Mahanti [19] offered an explanation, based on the formation of the dipole moment caused just by a pair of canted spins without the need to invoke magnetic structures such as that of spiral. Thus, this theory is a more general form of DMI explaining multiferroicity, adding an additional contribution to KNB coupling. Subsequently, Miyahara and Furukawa [24] proposed a microscopic model for such a local spin-pair-dependent electric polarization. In a nutshell, these theories [23,24] demand that multiferroicity can be observed in any canted antiferromagnet, owing to non-KNB coupling, apparently not restricted to $d$-metal ions. Clearly, NCL magnetic structures can present surprising situations in the field of magnetism [25]. Therefore, there is a need to search for materials for new anomalies involving canted spins in general to advance the knowledge in the field of multiferroics. This is the motivation of the present work.

In this Rapid Communication, we provide an evidence in a globally centrosymmetric material for a spin-driven polarization mechanism. The conclusion is based on the neutron powder diffraction (NPD) studies on $Tb_2BaNiO_5$ (space group: *Immm*; see Supplemental Material in Ref. [27] for crystal structure), which was recently shown to be an "exotic" multiferroic below 25 K [26]. Density functional theoretical (DFT)

*Corresponding author: sampathev@gmail.com

 

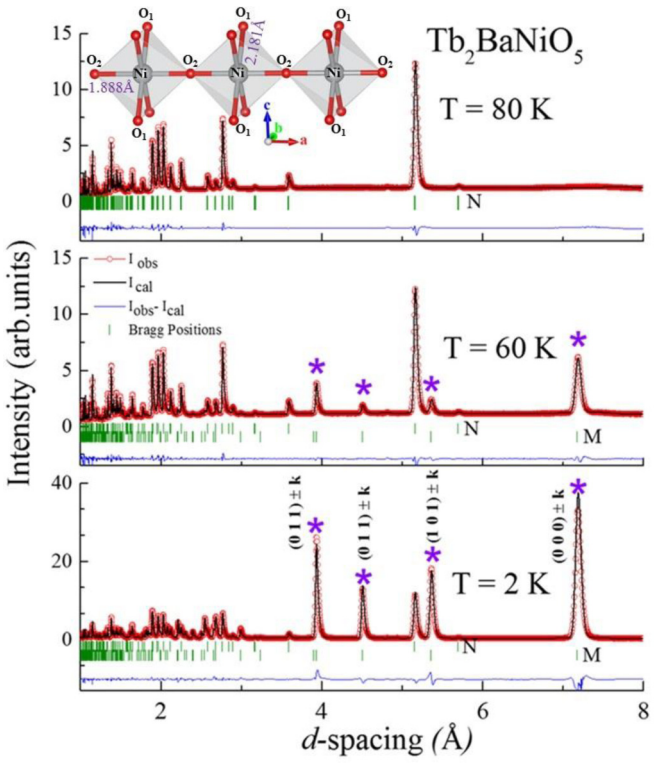


FIG. 1. Rietveld refinement of neutron-diffraction patterns of $Tb_2BaNiO_5$ at selected temperatures. Inset shows the $NiO_6$ chains running along the $a$ axis. In the bottom panel, the ($hkl$) values for magnetic Bragg peaks where $k = (1/2,\ 0,\ 1/2)$ are shown. Asterisks mark magnetic peaks. Nuclear (N) and magnetic (M) peak positions are shown by vertical green ticks.

calculations were carried out to support a canted magnetic ground state, derived from NPD.

The compound under investigation is a derivative of a spin-chain compound, $Y_2BaNiO_5$ [28], in which $Y$ is nonmagnetic. The spin chain, running along the $a$ axis (inset, Fig. 1), is made up of integer spins of Ni and hence this $Y$ compound is characterized by a gap between the nonmagnetic ground state and excited state (known as the Haldane gap). The interchain interaction is weak. In sharp contrast to this, when $Y$ is replaced by magnetic-moment-containing rare earths ($R$), antiferromagnetic (AFM) ordering gets triggered at both $R$ and Ni sites, interestingly, at the same temperature in the family $R_2BaNiO_5$. These compounds with a moment on $R$ are spin-driven multiferroics [26,29–31]. The magnetic structure is characterized [32,33] by the temperature-independent propagation vector $k = (1/2, 0, 1/2)$. The exotic nature of the Tb compound is due to the following: The Néel temperature ($T_N = 63$ K, also called $T_{N1}$ here) is the highest within this series and the observed value of magnetodielectric coupling (18%) is the largest ever reported for a polycrystalline compound, attributable to single-ion $4f$ orbital anisotropy [26]. In addition, this compound exhibits another subtle, but distinct magnetic anomaly at ($T_{N2} =$) 25 K which induces electric dipole ordering below this temperature only (and hence $T_{N2}$ is called the ferroelectric Curie temperature, $T_C$). Since no information about canting angle behavior across 25 K was presented in Ref. [32], we considered it absolutely essential to reinvestigate this compound by NPD carefully and to augment it with DFT calculations to throw light on the origin anomalies of this compound.

NPD experiments were carried out on a polycrystalline sample of $Tb_2BaNiO_5$ on a WISH diffractometer on the target station (TS-2) of the Rutherford Appleton Laboratory, UK. NPD patterns were obtained from 2 to 80 K in steps of 2 K. The FULLPROF [34] program was used to refine the nuclear and magnetic structures using the data measured in detector banks at average scattering angles ($2\theta$) of 27°, 58°, 90°, 122°, and 153° each covering 32° of the scattering plane. The electronic structure and magnetic ground state of $Tb_2BaNiO_5$ are obtained using the projector augmented plane-wave (PAW)-based method within the DFT framework as implemented in the Vienna Ab initio Simulation Program (VASP) [35]. The details of the methodology used in our calculations are given in the Supplemental Material [27].

The NPD pattern collected at $T = 80$ K was refined successfully for the orthorhombic structure in the space group $Immm$, in good agreement with the previous reports [28,31]. The details of the structural parameters are given in Table I of the Supplemental Material [27]. In Fig. 1, the observed ($I_{obs}$) NPD patterns along with refined profile ($I_{cal}$) are shown for $T = 2$, 60, and 80 K, which indicate good agreement. As expected, below $T_N$ (say, at ~60 K), additional peaks could be seen due to magnetic ordering, as known earlier [32,33]. These magnetic Bragg peaks could be indexed by invoking the propagation vector, $k = (1/2,\ 0,\ 1/2)$. The magnetic structure at 2 K resembles the model reported in the literature [32]. In fact, the magnetic structure of $Ho_2BaNiO_5$ was taken as the starting model for refinement [36]. As the temperature is lowered below 63 K, the magnetic Bragg peaks gain intensity due to the ordered moments of Tb and Ni. The magnetic structures at 2, 26, and 60 K are shown in Fig. 2. In the inset of Fig. 3(a), the variation in the magnitude of $\theta$ as a function of temperature is plotted for Ni and Tb magnetic moments. The angle here refers to the magnitude of the angle between the moment vector and the crystallographic (positive-direction) $c$ axis. The magnetic moment of Ni is canted in the entire $T$ range below $T_{N1}$, with the moment orienting almost along the $c$ axis at the onset of magnetic order. But $/\theta/$ increases with a gradual lowering of temperature, attaining a value of about 45° at 4.2 K. Thus, there is a large variation of $\theta$ of Ni moment below $T_{N1}$. However, the Tb moment is oriented close to the $c$ axis ($\theta = 1$ to 7°) at all temperatures with a weak $T$ dependence below $T_{N1}$. But, what is intriguing is that there is a sharp increase in the canted angle subtended by Ni with the $c$ axis at 25 K from about 18° in a narrow temperature interval reaching a saturation value below about 15 K. Naturally, the difference ($\Delta\theta$) in the canting angle of nearby Ni and Tb moments (oriented towards, say, the positive $c$ direction) increases sharply below this temperature [Fig. 3(a)]. There is a noticeable change in Ni/Tb magnetic moments (Fig. S2 in the Supplemental Material [27]). It is worth noting that the shape of the plot of $/\Delta\theta/$ [Fig. 3(a)] resembles the plot of electric polarization versus temperature, reported earlier (see Fig. 4(b) in Ref. [26]), thereby establishing a close correlation between these two.

It is to be noted that there are sudden changes at 25 K in the angles of O1-Ni-O1 and Ni-O1-Tb, as shown in Figs. 3(b)

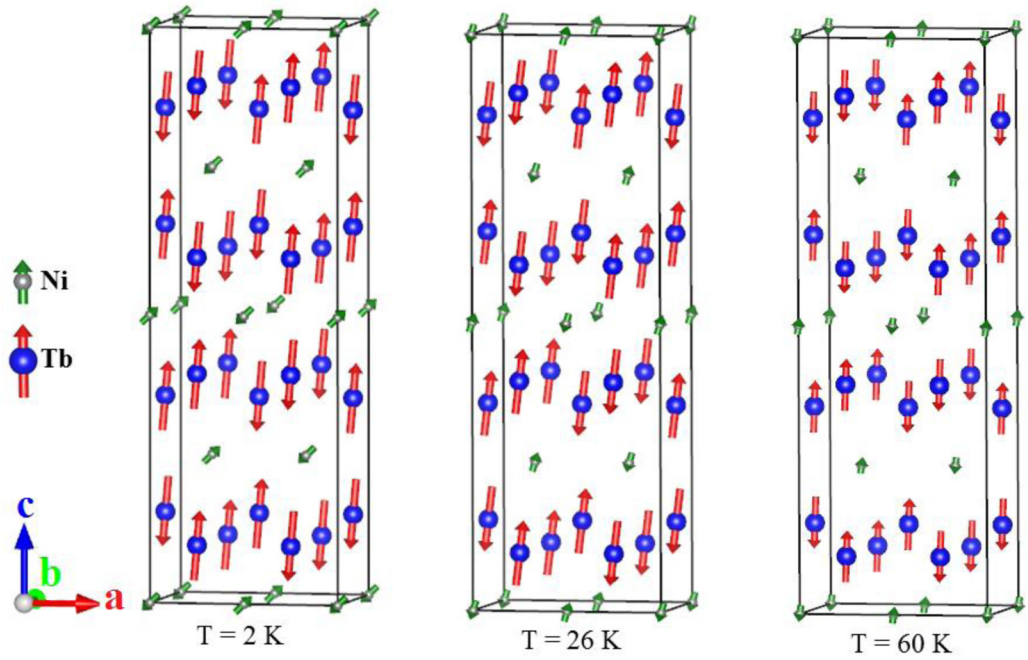


FIG. 2. Magnetic structure of $Tb_2BaNiO_5$ at selected temperatures. A $2\times1\times2$ supercell is shown here.

and 3(c). The O1-Ni-O1 bond angle remains steady around 78.905° up to 40 K, and, below 40 K it starts increasing gradually, peaking at 24 K. Below 24 K, it starts decreasing to around 78.895°. The overall change in the absolute values is small, but it is much bigger than the experimental errors. The Ni-O1-Tb bond angle also undergoes a change, with this angle increasing below 24 K.

We observed that the influence of coupled ordering at 25 K is felt in the lattice constants as well [Fig. 4(a)], determined from NPD patterns. The lattice constant $a$ increases, and $b$ and $c$ decrease with decreasing temperature, but exhibit sudden changes around 25 K. It may be noted that there is a gradual change of slope even near $T_{N1}$. Since it is more instructive to see how bond lengths are getting influenced at this temperature, we have plotted the $T$ dependence of bond lengths for Ni-O1 and Ni-O2 (lying along the chain, called "apical" distance in Ref. [32]) in Figs. 4(b) and 4(c). We can confidently state that the Ni-O1 bond length tends to show an upward trend below 25 K, with respect to the positive temperature coefficient seen above 25 K. There is, of course, an influence on Ni-O2 distances as well, in the sense that the slope value changes gradually around this temperature. A careful look at the analyzed data revealed that the $z$ value for Tb with the coordinate $(1/2,\ 0,\ z)$ exhibits a weak, but observable change in the vicinity of $T_{N1}$ as well as at $T_{N2}$, suggesting that Tb displacement possibly causes local electric polarization. On the basis of displacement, we infer that the local polarization along the $b$ direction is favored, rather than along the $c$ direction.

In short, the NPD data show that there is an apparent critical (*relative*) canting angle of Ni and Tb magnetic moments that has to be exceeded for electric dipole ordering to get triggered by magnetic order—which is a fascinating observation. As shown above, there is a weak, but sudden change in the bond distances and the bond angles subtended by magnetic moments with oxygen at 25 K. *These are the key findings of this experimental work, which was not reported in earlier NPD investigations* [32]. Note that the sublattice magnetic structure is of a collinear type for both Ni and Tb. In other words, there is no evidence for cycloidal magnetic structure, even when one enters the multiferroic region (that is, below 25 K), thereby raising a question on the applicability of conventional DMI-based models [16] to describe multiferroicity in this case. Even at $T_{N1}$, there is a lattice strain (possibly due to symmetric exchange from the intrasublattice collinearity), but it is still weaker, as inferred from a weak slope change in the plots of lattice constants versus temperature (Fig. 4), but the strain below 25 K only results in electric dipole ordering. This finding establishes that it is the large difference in local canting angles of Ni and Tb moments below 25 K that apparently results in a relatively enhanced lattice strain leading to net spontaneous electric polarization. These observations support the need for an exchange-striction-based model even to NCL magnetic insulators, also when a rare earth with well-localized magnetic moments (not favorable to superexchange interaction) is involved in interatomic canting to trigger multiferroicity. The "local spin-canting" theory of Ref. [19] appears to be more general in this respect (that is, without insistence of any spiral magnetic structure) and it is therefore of interest to extend this model to take into account exchange striction. (In the range 25–63 K, possible local electric dipoles created by canting appear to average out over a large volume, making the net spontaneous polarization zero). At this juncture, it is worth stating that our initial studies on $Tb_{2-x}Y_xBaNiO_5$, investigated up to $x = 1.5$, suggest that $T_{N2}$ and $T_C$ get reduced linearly with $x$ (Fig. S3 in the Supplemental Material [27]), almost scaling with the concentration of Tb. This finding favors local canting involving Tb $4f$ (consistent with the role of Tb, inferred from $z$-coordinate values as well above). Finally, we admit that we are not able to resolve noncentrosymmetry at

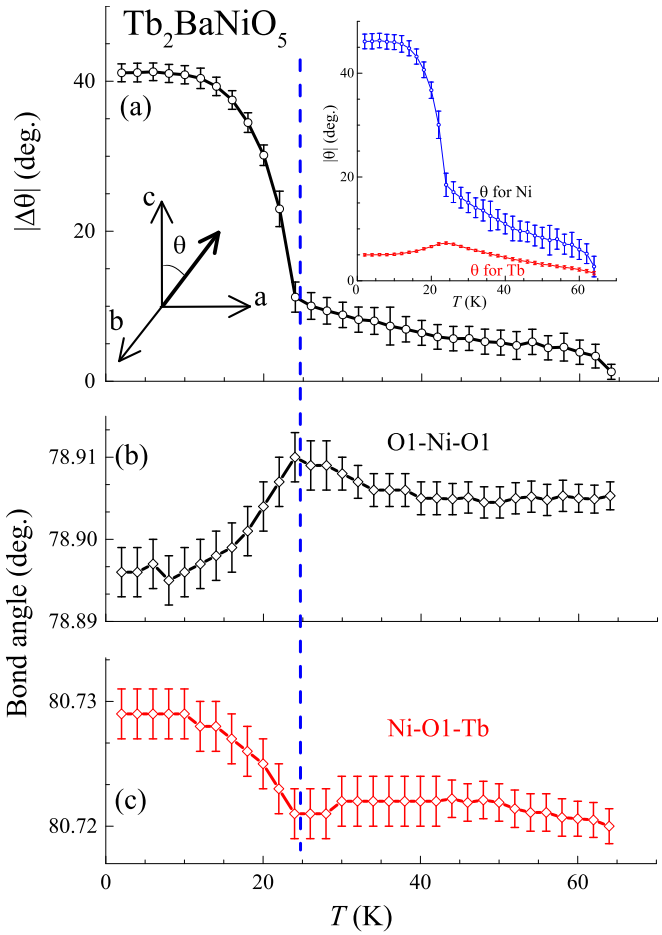


FIG. 3. (a) Temperature dependence of relative canting angles of Ni and Tb in $Tb_2BaNiO_5$ obtained from NPD data. In the inset, the magnitude of canting angles for a pair of Ni and Tb moments towards the positive $c$ axis is plotted. (b),(c) Temperature dependence of bond angles. The lines through the data points serve as a guide to the eye and a vertical dashed line is shown where sudden changes occur.

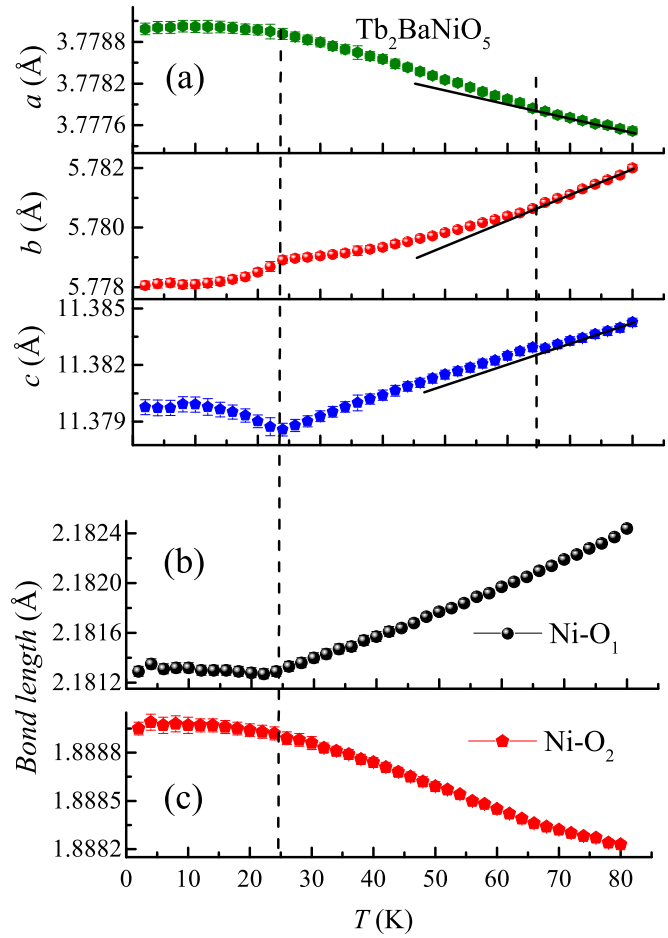


FIG. 4. (a) Temperature-dependent lattice parameters of $Tb_2BaNiO_5$ obtained from NPD data. Vertical dashed lines are drawn to show the temperatures at which magnetic features are seen. A dashed line is drawn through the data points above $T_N$ to show that there is a subtle, but gradual increase of lattice strain with decreasing temperature (as one enters the antiferromagnetic state). (b),(c) Bond lengths plotted as a function of temperature.

the onset of electric dipole order from the present NPD results. We reconcile this by the fact that the lattice distortions are so small that the resulting loss of inversion symmetry escapes detection in neutron and x-ray diffraction, as known for some other multiferroics, even in the recent past [37,38]. We are not, however, handicapped by this assumption to draw the present conclusions.

In order to render support to the magnetic state obtained from NPD, we carried out first-principles DFT calculations. The total-energy calculations were performed using the experimental structural parameters for various magnetic configurations (Fig. S4 in the Supplemental Material [27]) such as ferromagnetic (FM), ferrimagnetic, and different AFM orders including the one observed in experiments within generalized gradient (GGA), GGA + $U$, and GGA + $U$ + SO (where SO refers to spin-orbit) approximations. We noted that within the GGA + SO approximation, the electronic structure is metallic, which is not consistent with the experimentally observed insulating behavior of this spin-chain family. Therefore, a finite Coulomb correlation energy, $U$, is essential in the calculations. We further computed total energies assuming collinear and noncollinear spin configurations (with respect to the $c$ axis) for the AFM order observed experimentally (AFM-CL and AFM-NCL, respectively) within the GGA + $U$ + SO approximation. For the CL magnetic state, the magnetic moments of both Tb and Ni ions were fixed parallel to the $c$ axis. However, for the case of the NCL magnetic state, the magnetic moments of Ni ions were allowed to rotate in the $a$-$c$ plane; the Tb moments were fixed along the $c$ axis as neutron measurements show very small $\theta$ for Tb and the end results are not affected by such marginal changes. In the NCL case, the initial magnetic state with Ni moments canted at 45° with respect to the $c$ axis was allowed to relax over a self-consistency cycle until it reached the energy minimum. The value of $U_{\text{eff}} = U - J$ (where $U$ is the Coulomb correlation and $J$ is Hund's exchange) was varied systematically between 0 and 4.5 eV for Ni, while for Tb the values were fixed at 0 and at a value typical of heavy rare earths, e.g., 7 eV. Comparing total energies of various magnetic states including the CL and NCL magnetic states, we observe that within the GGA + SO approximation, the ferromagnetic state is the ground state. On

incorporating $U$, the ground state becomes noncollinear AFM, which is consistent with that found in the neutron-diffraction measurements described above. Further, when we vary $U_{\text{eff}}$ for Ni $d$ states (keeping $U_{\text{eff}}$ fixed at 7 eV for Tb $f$ states) up to a critical value of $U_{\text{eff}}$ for Ni (which is around 2 eV here), the ground state remains noncollinear. However, on increasing $U_{\text{eff}}$ beyond 2 eV, the CL magnetic state becomes the lowest-energy state (see Table II in the Supplemental Material [27]). From our NCL calculations, we have computed $\theta$ of the Ni moment (Table III and Fig. S5 in the Supplemental Material [27]) which are seen to increase with $U$ applied to Ni and, for $U_{\text{eff}} \geqslant 1.5$ eV, it lies in the range of 30°–40°, which are quite close to experimentally observed value at 2 K. Finally, we have fully optimized the experimental crystal structure for FM and AFM-CL configurations. Optimized structural parameters are listed in Table IV of the Supplemental Material [27]. We can clearly see that in the case of AFM-CL, the Ni-O-Ni bond angle along the chain (i.e., $a$ axis) is not exactly 180° as found in the case of FM, establishing local distortion.

In conclusion, this Rapid Communication brings out a situation in which a critical canting angle of a pair of spins (Ni $3d$ and Tb $4f$) determines the onset of magnetoelectric coupling. It is the existence of two different canted regimes below Néel order in a single compound that enables us to pose a question of whether the concept of a critical canting angle for such an adjacent pair of magnetic ions with favorable exchange striction, is relevant for multiferroicity. Additionally, it is worth noting that one of the pairs involved in canting contains a well-localized $4f$ orbital with nonzero orbital angular momentum, occupying a site different from the $d$ ion in the crystal structure, unlike in many other spin-driven multiferroics in which (spatially extended) $d$ orbitals occupying the same site cause multiferroicity. Dong *et al.* [39] recently emphasized the need to identify multiferroics in which $f$ moments play a key role to understand the role of spin-orbit coupling to mediate electric polarization. This Tb-based material could be a case to address this issue. In short, this work is a step forward in canted-spin-caused multiferroicity.

Neutron data taken at the ISIS Neutron and Muon Source. Information on the data can be accessed through STFC ISIS Facility [40].

E.V.S. would like to thank D. Khalyavin for his help during neutron-diffraction measurements, Ganapathy Vaitheeswaran for preliminary DFT calculations on simple ferromagnetic and antiferromagnetic structures, and K. Maiti for his comments on the manuscript. We thank the ISIS facility for providing beam time on WISH, RB1810006.

[1] D. Khomskii, Physics **2**, 20 (2009); J. van den Brink and D. I. Khomskii, J. Phys.: Condens. Matter **20**, 434217 (2008).
[2] N. A. Spaldin, S. W. Cheong, and R. Ramesh, Phys. Today **63**, 38 (2010).
[3] M. Fiebig, T. Lottermoser, D. Meier, M. Trassin, Nat. Rev. Mater. **1**, 16046 (2016).
[4] S. Dong, J.-M. Liu, S.-W. Cheong, and Z. Ren, Adv. Phys. **64**, 519 (2015)
[5] M. Fiebig, J. Phys. D: Appl. Phys. **38**, R123 (2005).
[6] G. A. Smolenskii and I. Chupis, Sov. Phys. Usp. **25**, 475 (1982).
[7] A. Filippetti and N. A. Hill, J. Magn. Magn. Mater. **236**, 176 (2001).
[8] O. Heyer, N. Hollmann, I. Klassen, S. Jodlauk, L. Bohaty, P. Becker, J. A. Mydosh, T. Lorenz, and D. Khomskii, J. Phys.: Condens. Matter **18**, L471 (2006).
[9] N. Hur, S. Park, P. A. Sharma, J. S. Ahn, S. Guha, and S.-W. Cheong, Nature (London) **429**, 392 (2004).
[10] T. Kimura, T. Goto, H. Shintani, K. Ishiazaka, T. Arima, and Y. Tokura, Nature (London) **426**, 55 (2003).
[11] G. Lawes, A. B. Harris, T. Kimura, N. Rogado, R. J. Cava, A. Aharony, O. Entin-Wohlman, T. Yildrim, M. Kenzelmann, C. Broholm, and A. P. Ramirez, Phys. Rev. Lett. **95**, 087205 (2005).
[12] T. Kimura, J. C. Lashley, and A. P. Ramirez, Phys. Rev. B **73**, 220401(R) (2006).
[13] Y. J. Choi, H. T. Yi, S. Lee, Q. Huang, V. Kiryukhin, and S.-W. Cheong, Phys. Rev. Lett. **100**, 047601 (2008).
[14] Y. Naito, K. Sato, Y. Yasui, Y. Kobayashi, Y. Kobayashi, and M. Sato, J. Phys. Soc. Jpn. **76**, 023708 (2007).
[15] M. Mostovoy, Phys. Rev. Lett. **96**, 067601 (2006).
[16] H. Katsura, N. Nagaosa, and A. V. Balatsky, Phys. Rev. Lett. **95**, 057205 (2005).
[17] I. A. Sergienko and E. Dagotto, Phys. Rev. B **73**, 094434 (2006).
[18] N. Terada, J. Phys.: Condens. Matter **26**, 453202 (2014).
[19] T. A. Kaplan and S. D. Mahanti, Phys. Rev. B **83**, 174432 (2011).
[20] J. Hu, Phys. Rev. Lett. **100**, 077202 (2008).
[21] A. B. Harris, T. Yildirim, A. Aharony, and O. Entin-Wohlman, Phys. Rev. B **73**, 184433 (2006).
[22] T. Arima, J. Phys. Soc. Jpn. **76**, 073702 (2007).
[23] C. Jia, S. Onoda, N. Nagaosa, and J. H. Han, Phys. Rev. B **76**, 144424 (2007).
[24] S. Miyahara and N. Furukawa, Phys. Rev. B **93**, 014445 (2016).
[25] E. Bousquet and A. Cano, J. Phys.: Condens. Matter **28**, 123001 (2016).
[26] S. K. Upadhyay, P. L. Paulose, and E. V. Sampathkumaran, Phys. Rev. B **96**, 014418 (2017).
[27] See Supplemental Material at http://link.aps.org/supplemental/10.1103/PhysRevB.99.100406 for the crystal structure, temperature dependence of magnetic moment values and structural parameters derived from neutron diffraction data, and magnetic structures considered and various parameters in DFT calculations.
[28] J. Darriet and L. P. Regnault, Solid State Commun. **86**, 409 (1993).
[29] T. Basu, V. V. Ravi Kishore, S. Gohil, K. Singh, N. Mohapatra, S. Bhattacharjee, B. Gonde, N. P. Lalla, P. Mahadevan, S. Ghosh, and E. V. Sampathkumaran, Sci. Rep. **4**, 5636 (2014).

[30] S. Chowki, T. Basu, K. Singh, N. Mohapatra, and E. V. Sampathkumaran, J. Appl. Phys. **115**, 214107 (2014).
[31] K. Singh, T. Basu, S. Chowki, N. Mohapotra, K. K. Iyer, P. L. Paulose, and E. V. Sampathkumaran, Phys. Rev. B **88**, 094438 (2013).
[32] E. Garcia-Matres, J. L. Martinez, and J. Rodriguez Carvajal, Eur. Phys. J. B **24**, 59 (2001).
[33] E. Garcia-Matres, J. L. Garcia-Munoz, J. L. Martinez, and J. Rodriquez Carvajal, J. Magn. Magn. Mater. **149**, 363 (1995).
[34] J. Rodriguez Carvajal, Physica B **192**, 55 (1993).
[35] G. Kresse and J. Furthmuller, Phys. Rev. B **54**, 11169 (1996).
[36] E. Garcia-Matres, J. Rodrguez-Carvajal, and J. L. Martinez, Solid State Commun. **85**, 553 (1993).
[37] Q. Zhang, K. Singh, F. Guillou, C. Simon, Y. Breard, V. Caignaert, and V. Hardy, Phys. Rev. B **85**, 054405 (2012).
[38] A. Gauzzi, F. Milton, V. Pascotto Gastaldo, M. Verseils, A. Gualdi, D. Dreifus, Y. Klein, D. Garcia, A. J. A de Oliveira, P. Bordet, and E. Gilioli, arXiv:1811.07182, and references therein.
[39] S. Dong, H. Xiang, and E. Dagotto, Natl. Sci. Rev. (2019), doi:10.1093/nsr/nwz023.
[40] https://doi.org/10.5286/ISIS.E.RB1810006